Pluggable Silicon Photonic MEMS Switch Package for Data Centre

How Yuan Hwang[1], Jun Su Lee[1], Johannes Henriksson[2], Kyungmok Kwon[2], Tae Joon Seok[3], Ming C. Wu[2], Peter O'Brien[1]
[1]Tyndall National Institute, Cork, Ireland T12 R5CP
[2]Department of Electrical Engineering and Computer Sciences, University of California, Berkeley, CA 94720, USA
[3]School of Electrical Engineering and Computer Science, Gwangju Institute of Science and Technology, South Korea

E-mail: howyuan.hwang@tyndall.ie

Abstract

Consumers' thirst for data has led to the development of various silicon photonic switching devices that are highly scalable while maintaining their relatively compact form factor at the same time. This demands a paradigm shift in the way these devices are being packaged, as optical and electrical ports are involved. In this article, we proposed a pluggable silicon photonic MEMS switch package with passive optical coupling assembly. This approach shifts fibre coupling away from the package, keeping it "purely electrical." The pluggable concept is separately demonstrated through spring contacted hybrid assembly and pairs of vertically stack surface gratings. Insertion losses are comparable to planar fibre-to-grating coupling, with relatively broadband transmission and assembly tolerance.

Introduction to Silicon Photonic MEMS Switch

The growth in data traffic has led to development of innovative silicon photonic switching architecture such as electro-optic [1], thermo-optic [2] and MEMS [3] switches. The largest switch demonstrated so far is 128 x 128 ports by University of California, Berkeley [4] using row/column addressing approach from [5], consisting of 16384 switching cells. The unit cell of the switch is shown in Fig. 1.

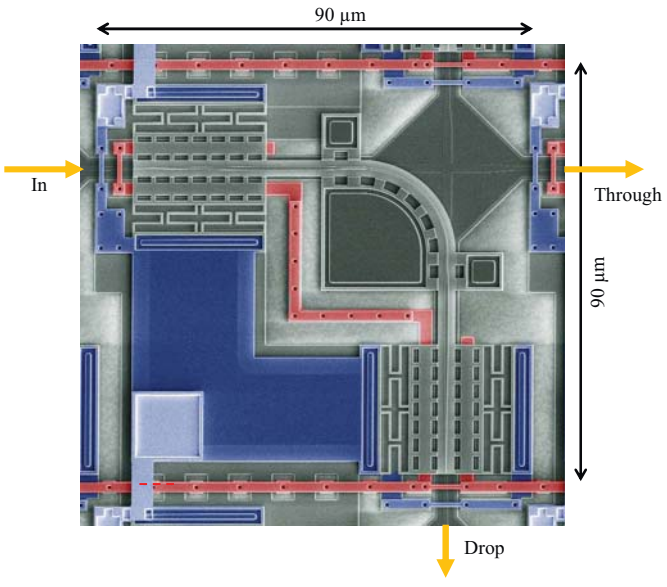

Fig. 1. Unit cell of the 128 x 128 silicon photonic MEMS switch [4].

Proposed Pluggable Concept

The authors have previously demonstrated various silicon photonic MEMS switch packaging schemes using via-less ceramic [6] and through glass via [7] interposers, steadily expanding the packaged switch ports from 12 x 12 to 128 x 128. However, in both demonstrations, the optical ports were still actively coupled and permanently fixed with optical resins onto the switch devices using lidless 64-channel regular fibre array and a pair of pitch-reducing 128-channel ion-exchanged optical interposers respectively. Such permanently fixed configurations are less cost-effective and efficient from end users' perspectives, as the whole structure – device, fibre, board, electronics and mechanical components have to be replaced should failure occurs.

In this follow-up development, the authors proposed a pluggable configuration mimicking a computer processor, but for both optical and electrical connections. This configuration reduces a silicon photonic package to "purely electrical", with fibre, electronics and mechanical components permanently placed on the motherboard. Fig. 2 shows the proposed pluggable concept using pairs of surface gratings. For polarisation independent coupling, on-board polymer waveguides can be used to edge-couple into inverted tapers on active photonic devices.

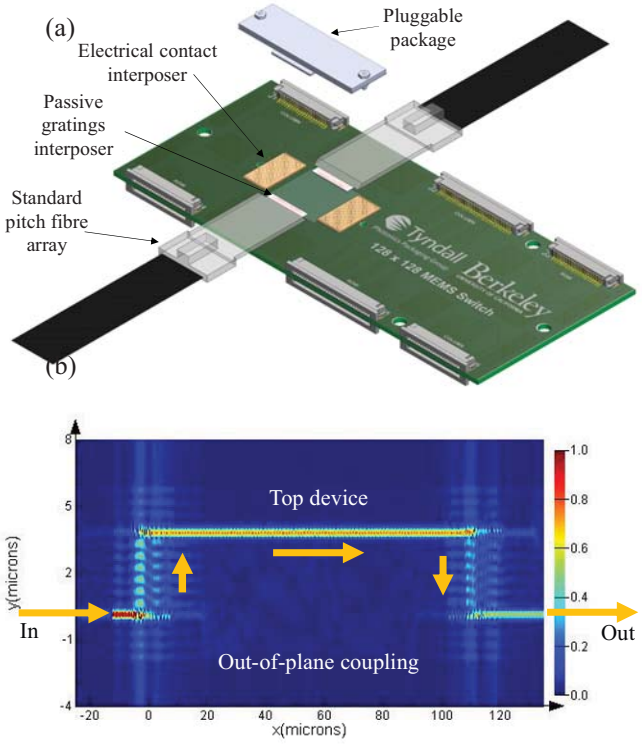

Fig. 2. (a) Proposed pluggable configuration, consisting of a "purely electrical" silicon photonic package and optical board and (b) Lumerical FDTD simulation of out-of-plane coupling using two pairs of non-uniform gratings.

Aside from the practicality of having a versatile pluggable package against a permanently fixed one from end users' perspective, this concept also eliminates the need of a reflow-able fibre-attached photonic package from packaging foundries. Fibre-to-optical interface couplings are highly sensitive to temperature variations and are commonly the last step to be assembled once all thermal processes are completed. In order for a fibre-attached photonic package to be reflow-able, specialty optical resin and fibres are needed, such as that demonstrated by [8].

While the concept is currently devised for a photonic MEMS switch, it can be readily expanded to other photonic systems, particularly in the field of medical and sensing applications, whereby photonic devices are typically meant for single use only. In this article, the pluggable concept is separately demonstrated with electrical and optical test vehicles in the following sections.

Electrical Packaging

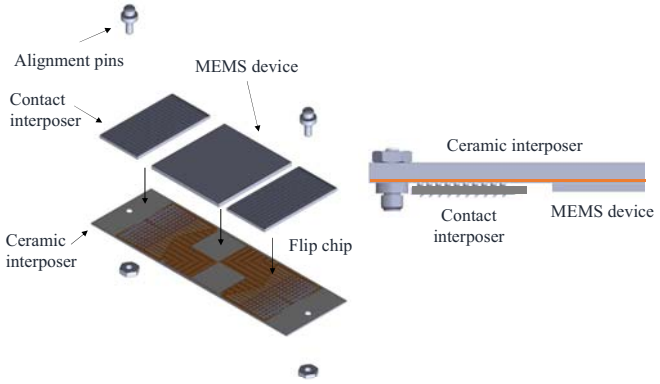

Fig.3. Pluggable silicon photonic package concept.

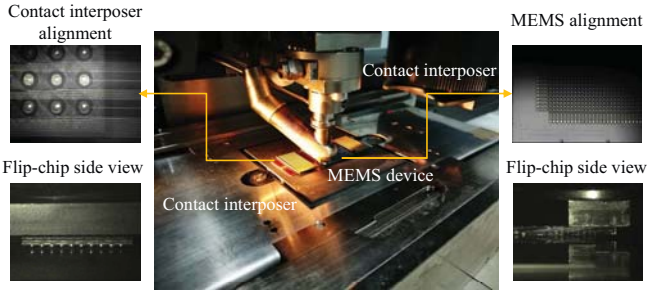

Fig. 4. Process integration of the pluggable package.

For electrical packaging, the pluggable concept is achieved through the use of off-the-shelf contact interposer [9] and via-less ceramic interposer. The design and overall concept is shown in Fig. 3. Two holes were integrated on the ceramic interposer for the alignment pins, while electrical ports from the MEMS switch are routed to two opposing edges and coupled into the contact interposers. Fig. 4 shows the process integration of the pluggable assembly and Fig. 5 shows the board level demonstration. Fig. 6 further compares the daisy-chained loop electrical resistance between the developed pluggable assembly and the previously demonstrated through glass via test vehicle from [7]. It can be seen that the via-less interposer used in current demonstration led to almost 4 times higher electrical resistance and has to be considered for future iterations.

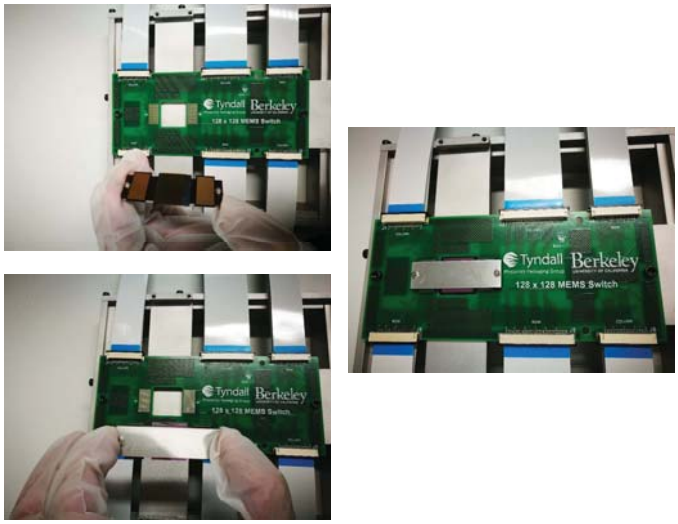

Fig. 5. Board level demonstration of the pluggable package.

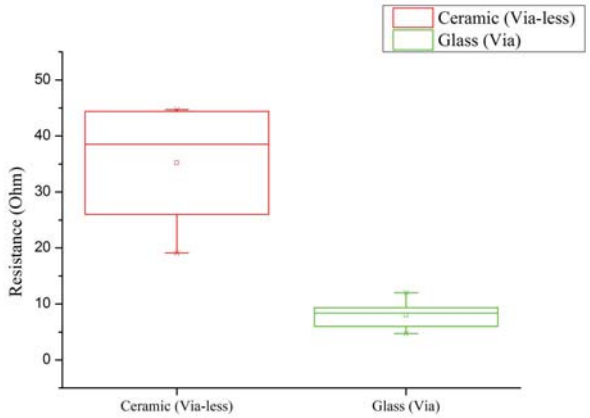

Fig. 6. Electrical resistance comparison between the via-less ceramic interposer versus through glass via interposer from [7].

Optical Packaging

[10], [11] had previously demonstrated that a pair of vertically stacked SOI grating couplers interacts in the same way a pair of grating-to-fibre behaves. [12] had also recently demonstrated that coupling between two different material systems is possible. These behaviours thus allow the development of a separate optical interposer and re-routing of optical waveguides becomes possible, similar to an electrical interposer that fans out the electrical transmission lines. The active photonic device can thus be kept as small as possible. This is attractive from packaging perspective as active runs in front end foundries can be up to 5.6 times more expensive than passive runs [13], [14].

At the same time, foundries have more or less perfected the design and processing of optical gratings in the form of process design kit (PDK) and can be made available to requestors following a non-disclosure agreement (NDA) execution. Moreover, having a separate optical interposer allows the use of lower cost fibre array at standard 127 μm or

250 µm rather than pitch-reducing types. Large number of optical ports can also be efficiently separated into smaller groups that are more easily coupled by smaller fibre array.

2D-FDTD simulations was first performed to compare the insertion losses per facet between fibre-to-gratings and gratings-to-gratings (proximity) systems using existing designs from literatures [15], [16]. Same air gap separation of 62.5 µm between the interfaces were assumed, and the results are plotted in Fig. 7. It can be seen that non-uniform gratings are better suited for proximity coupling with comparable insertion losses to fibre couplings.

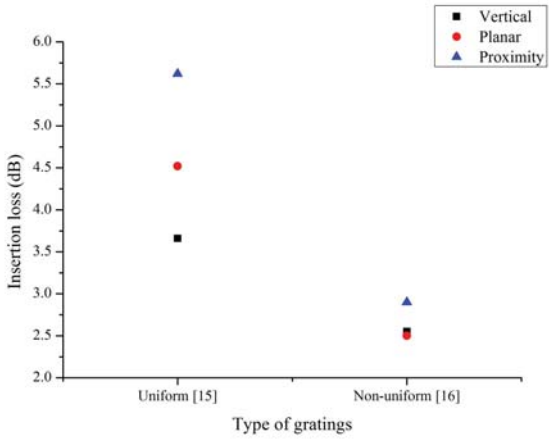

Fig. 7. 2D-FDTD simulation comparing insertion losses of fibre-to-gratings and proximity coupling. Asymmetric and symmetric mode profiles from uniform and non-uniform gratings affect insertion losses.

Next, in order to experimentally demonstrate the suitability of optical proximity for pluggable concept, the following test vehicle was prepared. Fibre-to-fibre transmissions of the test structures were first measured to be 2.2 dB (vertical fibre) and 2.68 dB (planar fibre) per facet. Next, only one facet of the grating test structures was coupled with a planar fibre. One of these samples was then flipped above the other with the opened facets facing each other (Fig. 8).

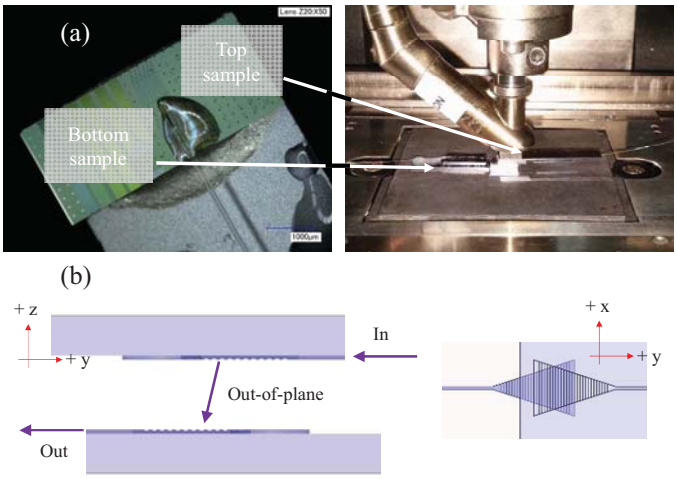

Fig. 8. (a) Measurement test vehicle, with the opened grating facets of the samples facing each other. (b) Orientation of the tolerance scan.

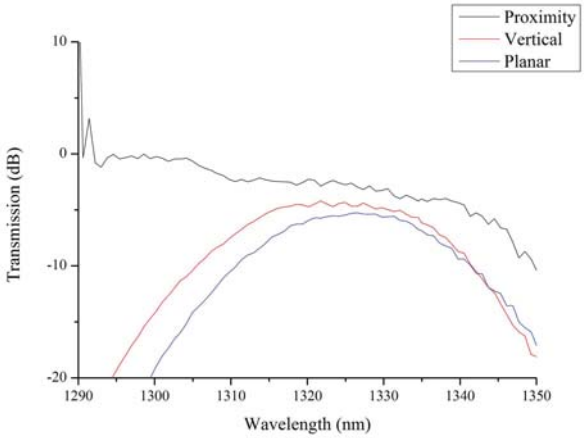

Fig. 9. Transmission spectrum between a pair of vertically stacked gratings that is relatively broadband compare to fibre-grating transmission.

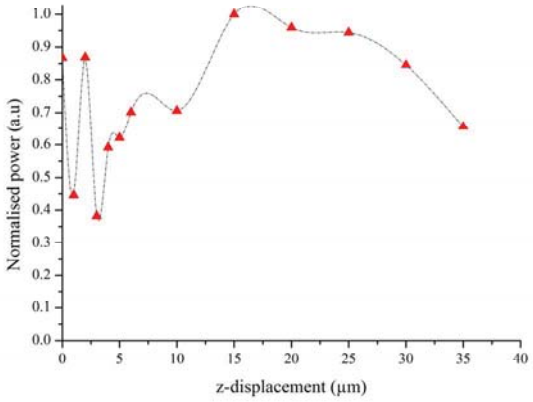

Fig. 10. Insertion loss between a pair of vertically stacked gratings in the vertical (z-) direction. Near-field oscillation below 10 µm separation can be seen.

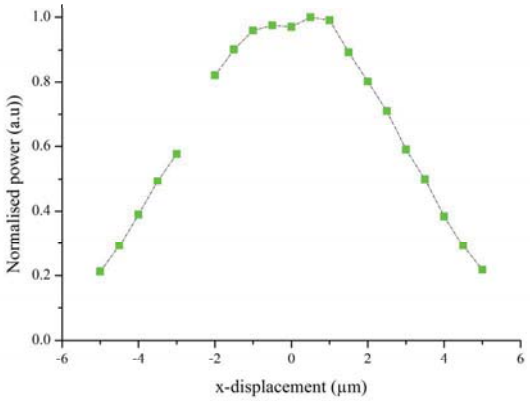

Fig. 11. Insertion loss between a pair of vertically stacked gratings in the across (x-) direction at z = 20 µm.

Experimental results showed that the insertion losses between a pair of gratings (3.18 dB at 1327 nm) were inherently higher than a pair of fibre-to-grating (vertical – 2.2 dB, planar – 2.68 dB) and this can be attributed to the fact that gratings were currently optimised for fibre coupling. The

results also matched that of the behaviour seen from Fig. 7 earlier.

Its broad bandwidth behaviour is however of particular interest, especially when being plotted alongside typical fibre-to-fibre transmission spectrums (Fig. 9). The tilt seen was due to imperfect roll/yaw/pitch angles of the top sample during experiments. Tolerance scan in the vertical (z-), across (x-) and along (y-) directions were then performed, analysed at 1327 nm and plotted in Figs. 10-12. Fig. 10 showed that an optimum vertical (z-) separation of 15 µm and a near-field oscillation below 10 µm separation, while Figs. 11-12 showed a 3 dB (50 %) alignment tolerance of approximately 7 µm in the across (x-) and along (y-) directions.

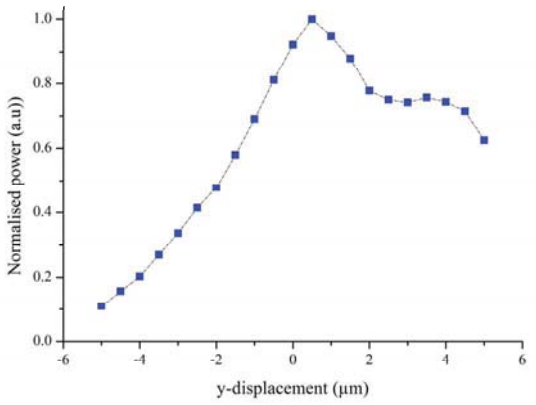

Fig. 12. Insertion loss between a pair of vertically stacked gratings in the along (y-) direction at z = 20 µm.

Conclusions

The authors have proposed a pluggable concept meant for silicon photonic MEMS switch device and have separately demonstrated how the electrical and optical ports can be coupled. This concept provides an alternative to the way photonic devices can be packaged, and more works are necessary to optimise the insertion loss between a pair vertically stacked gratings and improve the alignment tolerance further for future applications.

Acknowledgments

This project is a collaboration between the Center for Integrated Access Network (CIAN), United States and the Irish Photonics Integration Center (IPIC), Ireland. The packaging activity has been supported by Science Foundation Ireland (SFI) under grant number 12/RC/2276.

References

1. Yang, M., Green, W. M. J., Assefa, S., Van Campenhout, J., Lee, B. G., Jahnes, C. V., Doany, F. E., Schow, C. L., Kash, J. A., Vlasov, Y. A., "Non-blocking 4 × 4 Electro-Optic Silicon Switch for On-chip Ohotonic Networks", *Opt. Exp.*, vol. 19, no. 1, pp. 47-54, Jan. 2011.
2. Nakamura, S., Yanagimachi, S., Takeshita, H., Tajima, A., Hino, T., Fukuchi, K., "Optical Switches Based on Silicon Photonics for ROADM Application", *IEEE J. Sel. Topics Quantum Electron.*, vol. 22, no. 6, pp. 185-193, Nov./Dec. 2016.
3. Seok, T. J., Quack, N., Han, S., Muller, R. S., Wu, M. C., "Highly Scalable Digital Silicon Photonic MEMS Switches", *J. Lightw. Technol.*, vol. 34, no. 2, pp. 365-371, Jan. 2016.
4. Kwon, K., Seok, T. J., Henriksson, J., Luo, J., Ochikubo, L., Jacobs, J., Muller, R. S., Wu, M. C., "128×128 Silicon Photonic MEMS Switch with Scalable Row/Column Addressing," *Conference on Lasers and Electro-Optics (CLEO)*, 2018.
5. Quack, N., Seok, T. J., Han, S., Muller, R. S., Wu, M. C., "Scalable Row/Column Addressing of Silicon Photonic MEMS Switches," *IEEE Photonics Technology Letters*, Vol. 28, No. 5, p. 5610564, 2016.
6. Hwang, H.Y., Lee, J. S., Seok, T. J., Forencich, A., Grant, H. R., Knutson, D., Quack, N., Han, S., Muller, R. S., Papen, G. C., Wu, M. C., O'Brien, P., "Flip Chip Packaging of Digital Silicon Photonics MEMS Switch for Cloud Computing and Data Centre," *IEEE Photonics Journal*, Vol. 9, No. 3, June 2017.
7. Hwang, H. Y., Morrissey, P., Lee, J. S., Henriksson, J., Seok, T. J., Wu, M. C., O'Brien, P., "128 x 128 Silicon Photonic MEMS Switch Package Using Glass Interposer and Pitch Reducing Fibre Array," *IEEE 19th Electronics Packaging Technology Conference (EPTC)*, pp. 1-4, 2017.
8. Doerr, C., Heanne, J., Chen, L., Aroca, R., Azemati, S., Ali, G., McBrien, G., Chen, L., Guan, B., Zhang, H., Zhang, X., Nielsen, T., Mezghani, H., Mihnev, M., Yung, C., Xu, M., "Silicon Photonics Coherent Transceiver in a Ball-Grid Array Package," *2017 Optical Fiber Communications Conference*, Th5D.5.
9. Samtec Zray, https://www.samtec.com/connectors/high-speed-board-to-board/high-density-arrays/zray.
10. Yao, J., Zheng, X., Li, G., Shubin, I., Luo, Y., Thacker, H., Mekis, A., Pinguet, T., Sahni, S., Raj, K., Cunningham, J. E., Krishnamoorthy, A. V., "Grating-Coupler-Based Optical Proximity Coupling for Scalable Computing Systems," *Proc. SPIE 7944, Optoelectronic Interconnects and Component Integration XI, 794405*, January 17, 2011.
11. Bernabé, S., Kopp, C., Volpert, M., Harduin, J., Fédéli, J-M., Ribot, H., "Chip-to-chip Optical Interconnections Between Stacked Self-aligned SOI Photonic Chips," *Opt. Express 20*, 7886–7894, 2012.
12. Passoni, M., Floris, F., Hwang, H. Y., Zagaglia, L., Carroll, L., Andreani, L. C., O'Brien, P., "Co-optimizing Grating Couplers for Hybrid Integration of InP and SOI Photonic Platforms," *AIP Advances 8,* 095109, 2018.
13. Europractice, http://www.europractice-ic.com/docs/180517_MPW2018-general-v6.0.pdf
14. AIM Photonics, http://www.aimphotonics.com/mpw/
15. Grating coupler 2D-FDTD, Lumerical Knowledge Base, 2017. https://kb.lumerical.com/en/pic_passive_grating_coupler_2d.html
16. Chen, X., Li, C., Fung, C. K. Y., Lo, S. M. G., Tsang, H. K, "Apodized Waveguide Grating Couplers for Efficient Coupling to Optical Fibers," *IEEE Photonics Technology Letter*, Vol. 22, No. 15, 2010.